EMC Phenomena in HEP Detectors: Prevention and Cost Savings

F. Arteche
Imperial College, University of London
CERN, CH-1211 Geneve 23, Switzerland
C. Rivetta
SLAC, Stanford, CA 94025, USA

This paper addresses electromagnetic compatibility (EMC) studies applied to high-energy physics (HEP) detectors. They are focused on the quantification of the front-end electronic (FEE) sensitivity to conductive noise coupled through the input/output cables. Immunity tests performed on FEE prototypes of both the CMS hadron calorimeter and the CMS silicon tracker are presented. These tests characterize the sensitivity of the FEE to common and differential mode noise coupled through the power cables and the slow control network. Immunity tests allow evaluating the weakest areas of the system to take corrective actions before the integration of the overall detector, saving time and important costs.

1. Introduction

The Compact Muon Solenoid (CMS) is one of the four high-energy physic experiments under construction at CERN for the Large Hadron Collider (LHC) accelerator. The CMS calorimeter is integrated combining several sub-detectors designed specifically to achieve different objectives in the process of particle identification and energy measurement. In each sub-detector, the by-products of particle collisions are converted to electrical signals which are amplified by the front-end electronics (FEE). Processed signals are transmitted via optical links from the sub-detectors to the acquisition system located 120 meters away. Part of this electronic system is located inside of a uniform magnetic field of 4 Tesla and operates under particle radiation.

Due to the optical data transmission, the front-end electronics inside the detector can be considered as an isolated system with the only galvanic connection to the exterior through the low voltage/high voltage power supply system and the slow control network. Power supply units will be located 20-40 meters away from the detector due to the harsh environment above mentioned. Although all the fast signals are transmitted from the FEE to the acquisition system by optical fiber, a large amount of electromagnetic interference (EMI) exists in the detector among the electronic sub-systems.

Grounding and shielding policies and EMC plans have been addressed by the experiments designed for the LHC [1]-[4]. They consider everything from ground layouts, to define an equi-potential structure in the detector, to elaborated tests to quantify the FEE susceptibility to conductive noise perturbations. This paper presents results of immunity tests conducted on CMS front-end electronics. This work analyzes the results and possible solutions to improve the immunity and robustness of the front-end electronics before the final design and integration. Additionally, the paper addresses the concepts behind the immunity tests, the definition of the set-up and the procedure to conduct those tests, emulating the real conditions.

2. Noise Coupling Mechanisms

With the design of *Application Specific Integrated Circuits* (ASIC) to process the signal generated by the detectors, more specific functions can be integrated and located near the detector. It simplifies the front-end electronic design by reducing the connection path between the detector and the electronics input, digitizing the signal at the front-end and transmitting the pre-processed data to the counting room via optical fiber. For the last generation of calorimeters, ASIC designs allowed signals to be sampled at 40MHz and transmitted 120 meters, from the detector to the counting room. Based on that topology, the front-end electronics can be considered as an isolated system with the only galvanic connection to the external part of the calorimeter through the power distribution and slow control network.

The minimum signal that the front-end electronics can process is determined by the noise level coupled to the system. In addition to the intrinsic thermal noise perturbing the input stages of the system, electromagnetic interferences degrade the noise performance of the FEE. Due to the bandwidth associated with the front-end electronics and the dimensions of the sensitive processing areas, the electromagnetic noise coupled to the FEE is caused by conductive and near field mechanisms. In this scheme, the total noise that degrades the performance of the FEE can be divided in four components:

1. Thermal noise

2. EMI picked up by Detector - FEE connection

3. EMI picked up by FEE - external connections

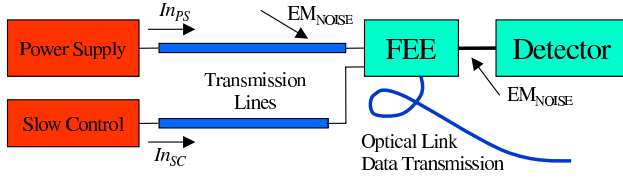4. Additional sources, as ADC quantization error, etc.

Figure 1: EMI and conductive noise coupled to the FEE.

Fig. 1 shows the coupling paths of the conductive noise and EMI perturbing a generic FEE.

Evaluating the signal plus noise at the ADC output at the sampling instants $t = kT$, it is

$$v_{ADC}(kT) = s(kT) + n_{total}(kT) \qquad \text{with } k = 1, 2, ...,$$

where T is the sampling period and $n_{total}(kT)$ is a random sequence defined by the contribution of the different noise sources at the ADC output. It is defined by

$$n_{total}(t) = n_{TH}(t) + n_{F-D}(t) + n_{F-E}(t) + n_{ad}(t),$$

where $n_{TH}(t)$, is the noise contribution due to the thermal noise generated at the input stage of the FEE; $n_{F-D}(t)$, EMI coupled in the connection detector-FEE, $n_{F-E}(t)$, EMI coupled to the FEE through the external connections and $n_{ad}(t)$, represents additional noise generated internally by the FEE. The $n_{F-D}(t)$ is particularly important when the detector and the FEE are located in different areas and relative long cables connect the detector to the FEE. $n_{F-E}(t)$ includes the perturbation due to conductive noise currents injected by auxiliary equipment, as power supplies, $I_{n_{PS}}(t)$, slow control, $I_{n_{SC}}(t)$, and EMI due to near and far EM field coupled by surrounding electronic systems.

The total noise defines the minimum signal $s(t)$ that can be processed by the FEE and the design goal focuses on minimizing the thermal noise and characterizing and reducing the effects of the EMI contributions. Assuming independence in the perturbations and using $\|.\|_2^2$ to quantify the power of the noise contribution, a criterion usually followed in HEP designs is to make the magnitude of the minimum signal processed $min(s_p)$ such that

$$\frac{min(s_p)}{\|n_{total}\|_2} \approx \frac{min(s_p)}{\|n_{TH}\|_2} >> 1,$$

forcing in the design $\|n_{F-D}\|_2^2 + \|n_{F-E}\|_2^2 << \|n_{TH}\|_2^2$. This relationship has to be enforced in all the stages of the front-end electronic design. It involves not only the careful design of the coupling between the detector and the FEE, to minimize $\|n_{F-D}\|_2$, but also the proper design of the distribution and slow control cables and shielding to reduce $\|n_{F-E}\|_2$. Considering

the volume and power involved in the new generation of calorimeters for LHC, a systematic approach must be followed to minimize the noise contribution due to EMI coupling into the FEE of the different sub-detectors of the whole calorimeter. The plan has to link safety considerations, to design the grounding topology, with immunity and radiation noise tests to quantify the effect of EMI in the front-end electronics.

3. EMC applied to the new generation of HEP detectors

A generic EMC plan to address the integration of HEP detectors should have these four basic steps:

- Power Supply distribution block diagram per sub-detector
- Grounding Scheme
- Immunity Tests
- Emission Tests

The power supply distribution block diagram per each sub-detector indicates the power level distributed in each sub-system and the current magnitude transmitted through the cables. This information is used to design the cable routing in a safe way and to group the bundles of cables based on power levels. Also, it is used to study possible failure scenarios in each sub-system and identify the power level involved in case of such failures. The grounding scheme of each sub-detector shows shields, enclosures and box connections, as well as the safety ground connection. The information obtained from this diagram will be used to verify electrical safety issues and identify possible ground loops and EMI sources/receptors. The immunity and emission tests are the most important part of the EMC plan. CMS have considered a set of EMC tests to quantify the immunity limits of each sub-detector to both conductive radio-frequency (RF) noise and transient signals. RF immunity tests characterize the sensitivity of the front-end electronics to differential and common mode noise coupled through the power cables, the slow control network and cable shields.

3.1. Immunity Tests

This paper addresses EMC studies focused on the quantification of the FEE sensitivity to RF conductive noise coupled through the input/output cables. It presents results of immunity tests performed on FEE prototypes of both the CMS hadron calorimeter and the CMS silicon.

Based on the previous analysis, the noise contribution $n_{F-E}(t)$ can be minimized by reducing both
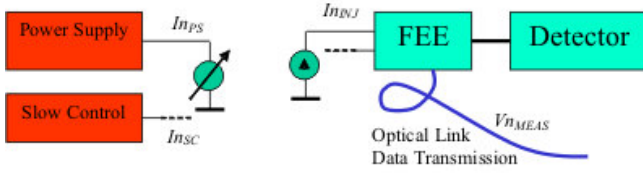
Figure 2: RF immunity and emission tests.

Figure 3: Set-up prepared to measure RF immunity.

the perturbing currents, $I_{n_{PS}}(t)$, $I_{n_{SC}}(t)$, and the EM_{NOISE} and improving the immunity of the FEE to such perturbations. Those magnitudes can be quantified to reach an optimal improvement considering costs and performance. Assuming deterministic perturbations, the noise contribution $n_{F-E}(t)$ in frequency domain can be expressed generically as

$$n_{F-E}(\omega) = S_{PS}(\omega)I_{n_{PS}}(\omega) + S_{SC}(\omega)I_{n_{SC}}(\omega) + ...,$$

where $S_i(\omega)$ represent the sensitivity of the front-end electronics to the noise coupled through the ith port.

The sensitivity function can be measured injecting perturbing currents to the FEE at different frequencies through the input power cables and slow control network and measuring the noise coupled to the sensitive electronics. This procedure is shown in Fig. 2. Results are evaluated to identify the coupling mechanism between the injected noise and the sensitive areas of the FEE. This information is used to characterize the immunity of the system to RF perturbations defining weak points in the design and additionally, to provide data to define the emission level to be imposed to the auxiliary equipment connected to the front-end electronics. Complementary emission tests are performed on the auxiliary equipment to validate the overall compatibility of the system (Fig. 2).

3.1.1. Methodology

RF immunity tests consist in injecting common-mode and differential-mode currents to the FEE at different frequencies through the input power cables, shields and slow control network and measuring the total output signal using the acquisition system of the sub-detector. These tests are performed before the power distribution cables, slow control network and final power supplies are fully specified. To estimate the FEE immunity, the experimental setup is designed such that the FEE and the auxiliary equipment exhibit during the test a configuration as close as possible to the final one. The FEE and the auxiliary equipment are placed on a copper plane as suggested by the standard IEC-61000 [6]. This copper sheet is the reference ground plane. Common mode and differential mode sine-wave currents are injected through the input power and slow control cables and shields using a bulk current injection probe [5]. The level of the injected signal is monitored using an inductive current clamp and a spectrum analyzer. To
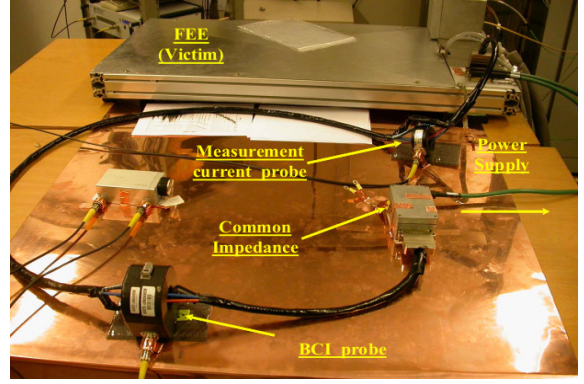
represent the effect of very long cables, normalized common impedances (common mode and differential mode impedances) based on lumped components are inserted between the power supplies and the FEE to standardize the measurements. The set-up used to perform the immunity tests in the CMS tracker is depicted in Fig. 3. The amplitude of the injected signal is compatible with a large signal-to-noise measurement and a linear operation on the FEE. The frequency of the injected current is changed between 150KHz to 50MHz. FEE output signal is measured using the acquisition system of the prototype. From Fig. 2, the RMS value of the measured output signal when the frequency of the injected noise is $f_i = \omega_i/2\pi$, becomes

$$\|V_{n_{MEAS}}(\omega_i)\|_2^2 \approx \|n_{TH}\|_2^2 + \|v_{ac}(\omega_i)\|_2^2 \qquad (1)$$

where $\|V_{n_{MEAS}}(\omega_i)\|_2$ is the total RMS signal at the FEE output and $\|v_{ac}(\omega_i)\|_2$ is the RMS value of the signal induced by the injected current $I_{nINJ}(\omega_i t)$. Based on these measurements, the FEE immunity at each frequency is defined by

$$S(\omega_i) = \frac{\|v_{ac}(\omega_i)\|_2}{\|i_{n_{INJ}}(\omega_i)\|_2}, \qquad (2)$$

where $\|i_{n_{INJ}}\|_2$ is the RMS value of the injected current at $f_i = \omega_i/2\pi$.

4. CMS Silicon Strip Tracker

Immunity tests were performed using the final prototype of the Silicon Tracker End-Cap (TEC) system to estimate the sensitivity of the FEE to conducted noise, evaluate the weakest areas of the sub-detector and take corrective actions before the integration of the overall system.

The detector module is the basic functional component of the silicon tracking system. Each module consists of three main elements: *1.- Single or*
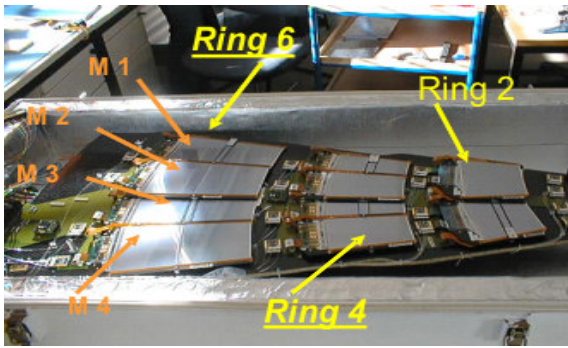
Figure 4: Silicon strip tracker petal used for conducting RF immunity tests.

Figure 5: Noise measured in ring 6 when CM noise currents are injected through the power cables.

double side silicon micro-strip sensors, 2.- Mechanical support (Carbon fiber frame), 3.- Readout front-end electronics (Hybrid circuit). These modules are grouped, partially overlapped, in rings and petals to cover several cylinders and the end-caps of the mechanical structure conforming the central tracker of CMS. Fig. 4 shows a picture of the TEC prototype used to perform the EMC tests, where both the module and the ring distributions of one petal are indicated. The prototype consists of a petal with 12500 channels and associated electronics distributed along one inter connection board (ICB).

The silicon tracker readout electronics processes analog signals from 10 million channels distributed across the silicon micro-strip detectors. It has four different parts: *1.- The micro-strip detector or sensor, 2.- The charge amplifier (APV25), 3.- The control unit, located in the detector, 4.- The front-end controller and front-end driver located in the counting room, 120 mts away from the detector.* Each micro-strip of the detector is read-out by a charge sensitive amplifier (APV25) [7] whose output voltage is sampled at 40 Msamples/sec. Samples are stored in an analogue pipeline for a few milliseconds and following a trigger signal, they are processed by an analogue circuit using a weighted sum algorithm to measure signal amplitude and the associated bunch-crossing to the hit. Processed data from different APV25 chips is multiplexed in time and sent over a short twisted pair cable to a laser diode, where electrical signals are converted to infrared light and transmitted over 120 mts. through optical fiber to the counting room, adjacent to the detector cavern.

The most sensitive component of the silicon tracker readout electronics is the charge amplifier. The APV25 is a 128-channel analogue pipelined custom chip used to read-out the silicon micro-strip detectors. Each channel is composed by a low noise amplifier, a 192-cell analogue pipeline and a de-convolution filter. The APV25 has two different operation modes, the peak mode (PEAK) and the de-convolution mode (DEC), with different bandwidths. For this sub-
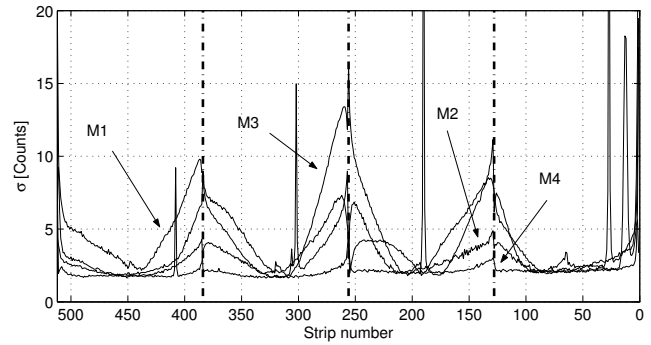
detector, the noise requirements set the overall thermal noise contribution of the APV25 amplifier in the system to a maximum of 2 counts RMS at the output of the ADC. It is equal to a noise of 1.64 mV RMS (1.22 counts/1 mV) or an equivalent RMS charge noise (ENC) at the input of the APV25 of 40 fC (2500 electrons). The prototype tested includes about 12500 channels and the output noise level spans between 0.8 and 2 counts RMS when no RF perturbation is injected. Further information about the TEC FEE can be found in [8].

Due to the distribution of the strip detectors and FEE in a large surface, the interference, affecting the prototype performance, depends on the amount of noise current coupled to the sensitive areas of the FEE. Due to slight differences in the connection between the modules and the ICB, the perturbing current does not affect equally all modules. Additionally, due to the particular connection between APV25 chips to the micro-strip detector, the noise does not distribute equally in all the APV25 channels. Partial results of the conducted noise tests performed are summarized in Fig. 5. This plot shows the raw signal per channel measured in the ring 6 of the prototype, when a common mode current at $10 MHz$ and $92 mA\ RMS$ is injected through the input power cables. This ring includes 4 modules composed each one by a 512-channel silicon strip detector and 4 APV25 chips. The perturbation is coupled unevenly into the modules. Those modules located near the inter connection board (ICB) are more sensitive to this perturbation. The noise also does not distribute equally across the 128 channels of each APV chip. The channels located close to the edge of the chip represent the worst case, while the one located close to the center of the chip are almost insensitive to the injected noise.

Based on the data previously collected, the sensitivity per channel to common mode currents flowing through the input power terminals of the TEC sub-detector is calculated by using (1) and (2). Fig. 6 shows the average sensitivity to common mode currents injected through the input power cables of the
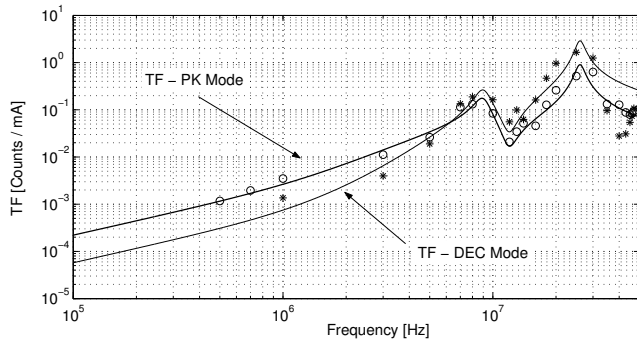
Figure 6: RF immunity to CM currents injected through the power cables.

Figure 7: RF immunity to CM currents injected through the monitoring cables.

50 worst channels of module 3, ring 6 of the Tracker Silicon Strip detector prototype . The resonances at 9MHz and 25MHz correspond to parasitic elements in the layout of the composite system Strip Detector-APV-Power Distribution. This curve allows us quantifying the sensibility of the FEE to common noise currents. They are used to understand the coupling mechanism between the external noise currents and the sensitive parts of the FEE and apply corrective actions in case of being necessary. The coupling mechanism depends on three factors; the APV inductance of the 1.25V distribution bus inside the chip, the resonance of the distribution circuit and the amount of perturbing current flowing though the sensitive areas. The common mode immunity of TEC front-end electronics can be improved if the APV inductance is minimized, the circuit resonances are controlled and the amount of noise current flowing through the input signal loop of the APV is reduced. From these three factors, at the moment, it is only possible to control the resonance reducing parasitic inductance and capacitance of the power distribution system and including in the final design common mode filters at the input power port to reduce the total amount of the common mode current coupled to the FEE.

Similarly, Fig. 7 shows the average immunity of Tracker Silicon Strip detector to common mode currents injected through the monitoring cables (slow control). From the results, the immunity can be improved placing common mode filters in the monitor lines.

5. CMS Hadron Calorimeter

Results of RF immunity tests conducted on a FEE prototype of the CMS Hadron Calorimeter (HCAL) are presented in this paper. In this prototype, the input amplifier is a custom chip whose design is based on a multi-range current splitter and gated integrator (QIE) [9]. This device amplifies and digitizes the signal generated by a hybrid photo-multiplier (HPD)
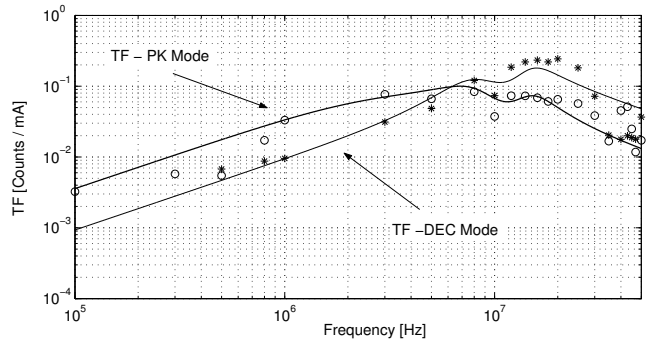
located a few centimeters from the amplifier. Parallel-digitized information is serialized and transmitted via optical fiber to the counting room by another ASIC chip. The FEE and the HPDs are housed in boxes containing between 50 and 72 channels. The front-end boards, the back-plane and the input power filter are placed into a metallic read-out box (RBX) that not only gives mechanical support to the electronic system but also EM shielding and thermal management. Further information about the HCAL FEE can be found in [10].

In the HCAL front-end electronics, each board contains 6 QIE chips and digital electronics to control the chips, serialize the data collected by the QIE's and transmit it to the acquisition system. The prototype used to perform the immunity tests consisted of 12 channels distributed in two identical boards, each of them connected to the back-plane. The target value for the thermal noise level of the QIE is 2.16 counts RMS at the output of the ADC or an Equivalent Noise Charge (ENC) at the input of the QIE equal to 0.72 fC (4500 electrons). In this prototype, the output noise level for all channels span from 2.64 to 2.94 counts RMS when no RF perturbation is injected.

Results of RF immunity tests conducted on the first prototype of the HCAL FEE are described below. Fig. 8 depicts the RMS value of the digitized voltage at the output of the QIE amplifier for all the channels, when the perturbing current is a sine wave whose frequencies are 5 MHz and 10 MHz with a magnitude of 6 mA RMS. In the same figure, the RMS value of the output voltages due to the injected current are compared with the RMS value of the output voltage noise of each channel when no perturbing signal is injected (Reference). The uneven distribution among channels of the noise injected is due to limitations of the grounding design in the HPD - QIE connection. Results of this measurements were used to improve the grounding and current return path at the level of the HPD board, in order to improve the noise immunity in those sensitive channels.

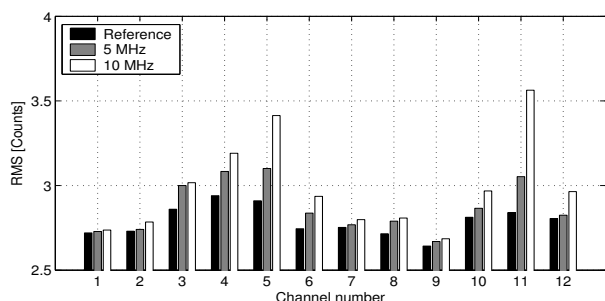Based on previous measurements and (1) and (2),

Figure 8: Noise measured in HCAL FEE when CM noise currents are injected through the power cables.
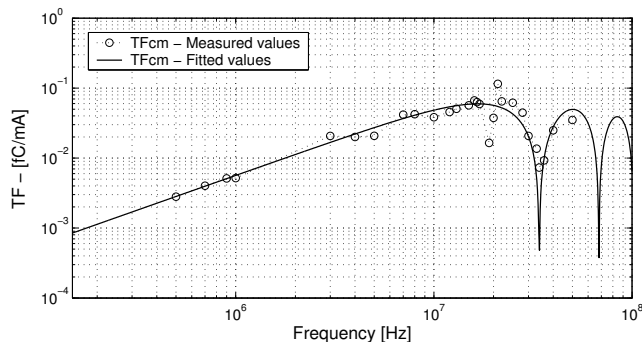

Figure 9: RF immunity of HCAL FEE to CM currents.

the sensibility function of the channel 5 measured between 500 kHz and 50 MHz is depicted in Fig. 4). These measured values can be fitted to a mathematical model representing the sensitivity function of the FEE to common mode currents. This model is proposed by combining the transfer function of the QIE with an additional term that models the coupling mechanism of the noise to the FEE. Notches at 36MHz, 72MHz, ... are associated with the finite integration time of the QIE.

6. Conclusions

Immunity tests to conductive noise have been conducted on prototypes of CMS sub-detectors. These tests quantify the susceptibility of the FEE and also identify the coupling mechanism between the injected noise and the sensitive areas of the system. Additionally, the immunity characteristic of the FEE allows defining the emission levels of the auxiliary equipment to be interconnected to that particular FEE. The proposed tests to quantify the FEE immunity to conductive noise and the emission levels of the auxiliary equipment sets a frame work to develop an EMC-based integration of HEP detectors. This information is used to define solutions improving the EM immunity of the system before final integration. Proposed solutions find some limitations that need to be evaluated in a frame of technical, risk and economic issues.

Acknowledgments

References

[1] F. Arteche, C. Rivetta and F. Szonsco, "Electromagnetic Compatibility Plan for the CMS Detector at CERN", Proc. of 15th Int. Zurich Symposium on EMC, February 18-20, 2003, Zurich, Switzerland, pp. 533-538.

[2] G. Blanchot, "Overview of the ATLAS Electromagnetic Compatibility Policy", Proc. 10th Workshop on Electronics for LHC, LECC 2004, pp 205-209, Boston, USA, Sept. 2004.

[3] J. Christiansen and V. Bobillier, "Grounding Issues for LHCb Experiment", http://lhcb-elec.web.cern.ch/lhcb-elec/html/grounding.htm .

[4] F. Formenti, "ALICE Grounding Plan", (TB 190602, draft), Personal Communication.

[5] S. Pignari and F. G. Canavero, "Theoretical Assessment of Bulk Current Injection versus Radiation", IEEE Trans. on EMC Vol 38, Issue 3, pp 469 - 477, August 1996,

[6] IEC - 61000-4-6 Electromagnetic compatibility (EMC) - Testing and measurement techniques Immunity to conducted disturbances, induced by radio-frequency fields," International Standard - Basic EMC publication Ed. 2000.

[7] M. Raymond, et. al., "The APV25 0.25 μm CMOS Readout Chip for the CMS Tracker", Proc. of IEEE Nuclear Science Conference, October 2000, Lyon, France, pp 113-118,.

[8] Katja Klein et. al. "The CMS Silicon Strip Tracker - Overview and Status", HEP2005 International Euro-physics Conference on High Energy Physics, Lisboa, Portugal, July 2005.

[9] T. Zimmerman and J. R. Hoff, "The design of a charge-integrating modified floating-point ADC chip", IEEE Journal of Solid-State Circuits, vol. 39, pp. 895-905, No. 6, June 2004.

[10] T. Shaw et. al, "Front-end readout electronics for the CMS hadron calorimeter," Proc. of IEEE Nuclear Science Conference, pp 194-197. Virginia, USA, November 2002.